Atmospheric CO2, CH4, and CO with CRDS technique at the Izaña Global GAW station: instrumental tests, developments and first measurement results

Angel J. Gomez-Pelaez[1], Ramon Ramos[1], Emilio Cuevas[1], Vanessa Gomez-Trueba[1,2], Enrique Reyes[1]

[1]Izaña Atmospheric Research Centre, Meteorological State Agency of Spain (AEMET), Tenerife, Spain.
[2]Air Liquide España, Delegación Canarias, Tenerife, Spain

Correspondence to: Angel J. Gomez-Pelaez (agomezp@aemet.es)

Abstract. At the end of 2015, a CO2/CH4/CO Cavity Ring-Down Spectrometer (CRDS) was installed at the Izaña Global Atmosphere Watch station (Tenerife, Spain) to improve the Izaña Greenhouse gases GAW measurement programme, and to guarantee the renewal of the instrumentation and the long-term maintenance of this programme. We present the results of the CRDS acceptance tests, the processing of raw data applied through novel numerical codes, and the response functions used. Also, the calibration results, the implemented water vapour correction, the target gas injection statistics, the ambient measurements performed from December 2015 to July 2017, and their comparison with other continuous in situ measurements are described. The agreement with other in situ continuous measurements is good most of the time for CO2 and CH4, but for CO is just outside the GAW 2-ppb objective. It seems the disagreement is not produced by significant drifts in the CRDS CO WMO tertiary standards. The main novelties are: 1) determination of a slight CO2 correction that takes into account changes in the inlet pressure/flow rate; 2) detailed justification of the use of virtual tanks to monitor the response function changes in time; 3) drift rate determination for the pressure and temperature sensors located inside the CRDS cavity; 4) novelties in the determination of the H2O correction for CO; and 5) determination and discussion of the origin of the CRDS-flow inlet pressure and H2O dependences.

1 Introduction

A CO2/CH4/CO CRDS (Cavity Ring-Down Spectrometer) was installed at the Izaña Global GAW (Global Atmosphere Watch) station (Tenerife, Spain) at the end of 2015 in order to improve the Izaña GHG (Greenhouse gases) GAW measurement programme, and guarantee the long-term maintenance of this programme. The incorporation of the CRDS technique for the measurement of atmospheric CO2, CH4, and CO mole fractions was a recommendation of the WMO World Calibration Centre WCC-Empa after its audit carried out at the Izaña Observatory in September 2013 (EMPA, 2013). The GAW programme of the World Meteorological Organization (WMO) requires high precision and accuracy in atmospheric GHG measurements, which are higher as higher the lifetime of the corresponding trace gas in the atmosphere is. The reason is that atmospheric GHG spatial gradients contain useful information about the spatial distribution of the surface

sources and sinks of these trace gases (Chevalier et al., 2010), but these gradients decrease in absolute value as the trace gas lifetime increases (Patra et al., 2014). The GAW required compatibility between laboratories is 0.1 ppm (parts per million in dry mole fraction) for carbon dioxide in the Northern Hemisphere and 0.05 ppm in the Southern Hemisphere; for methane, 2 ppb (parts per American billion in dry mole fraction); and for carbon monoxide, 2 ppb (WMO, 2015).

5   CRDS technique (Crosson, 2008) has improved considerably the stability and precision in the raw measurements compared to those of older techniques (e.g., NDIR -Non Dispersive InfraRed analysers-, GC-FID -Gas Chromatography with Flame Ionization Detector, and GC with RGD -Reduction Gas Detector-), being therefore the required frequency of use of calibrating/reference gases to achieve the GAW DQOs (Data Quality Objectives) much lower. Additionally, this spectrometric technique does not require chromatographic gases (e.g., carrier gas, make up gas, and FID gases for

10   maintaining the flame), which are expensive, and require great logistics efforts at remote stations. Zellweger et al. (2016) found out, when evaluating the results of scientific audit performed at GAW stations, that the results using newer spectroscopic techniques (CRDS and OA-ICOS -Off Axis Integrated Cavity Output Spectrometry), in general, are better than those obtained with older ones.

The Izaña Observatory (IZO) is a Global GAW station located at 2373 metres a.s.l. on Tenerife (Canary Islands, Spain),

15   usually above a strong subtropical temperature inversion. Since it is located at the summit of a mountain, during night-time there are North-Atlantic-free-troposphere background conditions, whereas during daytime there is a slight perturbation of these conditions by the arrival of an upslope thermal wind close to the terrain surface (e.g., Cuevas et al., 2013; Gomez-Pelaez et al., 2013; Rodríguez et al., 2009). Detailed information about the numerous measurement programmes operative at IZO are provided by Cuevas et al. (2015).

20   This paper presents the implementation of a CRDS G2401 at IZO and the independent development of novel Fortran 90 codes for raw data processing. The main novelties are: 1) determining a slight CO2 correction that takes into account changes in the inlet pressure/flow rate, and attributing it to the existence of a small spatial inhomogeneity in the pressure field inside the CRDS cavity; 2) detailed justification of the use of virtual tanks to monitor the response function changes in time; 3) providing equations to determine the drift rate of the pressure and temperature sensors located inside the CRDS

25   cavity; 4) introducing some novelties in the determination of the H2O correction for CO; and 5) physical determination and physical discussion the origin of the inlet pressure and H2O dependences of the CRDS flow.

The structure of this article is as follows. We firstly detail (Sect. 2) the results obtained in the initial tests performed to the Izaña CRDS (precision, repeatability, sensibility to inlet gas pressure, response function…) and the pre-processing applied to the raw data (Sect. 3). Secondly, we analyse the results of the calibrations performed every 3-4 weeks since the end of 2015

30   using Tertiary WMO standards, and provide some details on the response functions used and the numerical processing software developed to evaluate the calibrations (Sect. 4). Thirdly, some details of the obtained and implemented water vapour correction are provided (Sect. 5). Finally, the ambient measurements carried out till now are presented, as well as some details in the numerical processing software developed to obtain the ambient air CRDS measurements from raw data and calibration results, and compared with those obtained with other Izaña in situ measurement instruments (Sect. 6). In

Sect. 7, a preliminary independent assessment on the drift rates of the CRDS CO standards is performed. The main conclusions are outlined in Sect. 8. In Appendix A, a note concerning the inlet pressure and H2O dependences of the CRDS flow and the spatial inhomogeneity of the pressure field inside the CRDS cavity is presented. Additionally, we very briefly describe some few more novelties in the Izaña GHG measurement programme since GGMT-2015 (see Appendix B).

2 Acceptance tests performed to the CRDS

A Picarro G2401 CRDS analyser (CFKADS2196 serial number) for measuring CO2, CH4, CO and H2O was installed on November 2015 at IZO. Several acceptance tests were performed to the CRDS at the station, roughly following the recommendations provided by the European Integrated Carbon Observation System (ICOS)-Atmospheric Thematic Centre (ATC) (ICOS-ATC, 2016). For processing the data associated to the tests, the raw values for CO2 (not dry), CH4 (not dry), CO and H2O of the "Synchronized DataLog_User" files were used.

The first test was what ICOS calls a "Precision test", which consists in measuring a gas cylinder (filled with dry natural air) over 25 hours being the first hour rejected (stabilization time). As Table 1 shows, the results (standard deviations) obtained in this test were well within the threshold established by ICOS-ATC (2016).

Raw data average length	CO2 S.D.(ppm) Obtained/ICOS-threshold	CH4 S.D.(ppb) Obtained/ICOS-threshold	CO S.D.(ppb) Obtained/ICOS-threshold	Mean H2O (ppm)
1 minute	0.013 / 0.050	0.19 / 1.0	0.87 / 2.0	-2.8
60 minutes	0.009 / 0.025	0.14 / 0.5	0.16 / 1.0	-2.8

Table 1. Results obtained during the "Precision test" (see main text) and ICOS-threshold values for two average lengths (1 and 60 minutes). S.D. means "Standard Deviation".

The second test performed was a "Repeatability test". According to the ICOS terminology, it consists in measuring alternately a gas cylinder (filled with dry natural air) during 30 minutes and ambient air (not dried) during 270 minutes over 72 hours. Statistics are based only on the last 10-minute-average data for each gas cylinder "injection". Indeed, we used 2 cylinders, each one measured every 5 hours, with the following measurement cycle: cylinder 1 during 40 minutes, wet ambient air during 20 minutes, cylinder 2 during 40 minutes, and wet ambient air during 200 minutes. Table 2 shows the obtained results for each tank and 10-minute average period: 20-30 minutes and 30-40 minutes. The results were well within the threshold established by ICOS-ATC (2016)

Cylinder	10-minute average period	CO2 S.D.(ppm) Obtained/ICOS-threshold	CH4 S.D.(ppb) Obtained/ICOS-threshold	CO S.D.(ppb) Obtained/ICOS-threshold
1	20-30 min.	0.016 / 0.050	0.23 / 0.5	0.23 / 1.0

1	30-40 min.	0.021 / -	0.34 / -	0.28 / -
2	20-30 min.	0.016 / 0.050	0.23 / 0.5	0.35 / 1.0
2	30-40 min.	0.026 / -	0.31 / -	0.31 / -

Table 2. Results obtained during the "Repeatability test" (see main text) and ICOS-threshold values. S.D. means "Standard Deviation".

The third test performed was an ambient pressure sensitivity test of the measurements carried out for the mentioned period of 72 hours. The results obtained were: 0.4 ppb/10mb for CO, 0.038 ppm/10mb for CO2, and 0.47 ppb/10mb for CH4. Those sensitivities can be considered as small taking into account the GAW DQOs and the typical variation range of the atmospheric surface pressure.

The fourth test was an inlet pressure sensitivity test when measuring a gas cylinder filled with dry natural air. The cylinder air was continuously measured during more than 13 hours in two consecutive days, and the regulator low-pressure was changed alternatively between 8 psi and 2 psi, keeping the same pressure in the regulator during at least one hour each time. The sensitivities obtained were: 0.1 ppb/6 psi for CO, 0.04 ppm/6 psi for CO2, and 0.16 ppb/6 psi for CH4, which are quite small except for CO2. Since the CRDS inlet pressure can be slightly different (e.g., differences of a few psi may be present) when changing the sample (laboratory standards, target gases and ambient air), and in order to be able of achieving a very accurate response function for CO2, we empirically correct for this effect as explained in Sect. 3.1.

The fifth test was fitting response curves when calibrating with 4 WMO tertiary standards (6 cycles, 2.5 hours/cycle, each standard is measured during 30 consecutive minutes as well as a target gas). When performing a linear fitting for CH4, the Root Mean Square (RMS, accounting for the effective degrees of freedom) residual was 0.143 ppb (very small). When performing a linear fitting for CO, the RMS residual was 0.067 ppb (very small). However, when performing a linear fitting for CO2, the RMS residual was 0.0395 ppb, which is larger than the values we usually obtain with our NDIR-based measurement system for CO2 when using a quadratic fitting (Gomez-Pelaez & Ramos, 2011). Moreover, when using a quadratic fitting for the CRDS CO2, the RMS residual was 0.0284 ppm, still slightly worse than that of our NDIR-based systems. Finally, when correcting the raw CO2 from the inlet pressure sensitivity and then performing a quadratic fitting, the RMS residual was 0.0219 ppm, which is similar to the values obtained with our NDIR-based systems. During that first calibration, the inlet pressure differences were especially intense. We have improved our skills since then getting smaller inlet pressure differences during the calibrations.

3. Data acquisition and pre-processing

We call pre-processing to the computation of raw-data 30-second means and corresponding standard deviations using the DataLog_User files (no the synchronized ones), as well as to the computation of some derived variables. We have developed the pre-processing software in Fortran 90, as well as the calibration and ambient-air processing software. For the

computation of 30-second means and standard deviations, we take into account the so called "species" field (i.e., which informs about the fields that have been updated in each file line; there are 1.7 lines/second). The raw variables associated to each "species" value are: a) Species=1, CO_2, peak_14 (*p14*), and CO; b) Species=2, CH_4, CO_2_dry; c) Species=3, H_2O, h2o_reported (*hr*), CO_2_dry, and CH_4_dry; and d) Species=4, CO, b_h2o_pct (*bh*), and peak84_raw (*p84*); where CO_2 and CH_4 are raw values not corrected from H_2O dilution nor pressure broadening, whereas CO_2_dry and CH_4_dry have been (factory) corrected from those effects, *p14* is the raw value associated to the main CO_2 peak, CO is already (factory) corrected from the CO_2 and H_2O influences, H_2O is the calibrated value obtained from *hr*, which is the reported H_2O raw value associated to the main H_2O peak (in the CH_4-peak laser wavelength range), *bh* is the H_2O raw value associated to the secondary H_2O peak (in the CO-peak laser wavelength range), and *p84* is the raw value associated to the CO peak. Additionally, there are other raw variables not associated to a single "specie" value that we use: Cavity Pressure (*CP*), Cavity Temperature (*CT*), MPV Position (*MPVP*), Outlet Valve (*OV*), and Solenoid Valves (*SV*).

A 30-second mean is accepted when: a) at least 85% of the expected data is present; and b) all the instantaneous data have the same *MPVP* and *SV* values. Additionally, a counter called *npcmc* is assigned to each 30-second mean. It indicates the number of consecutive 30-second means with the same configuration for both, *MPVP* and *SV*.

3.1 Inlet pressure sensitivity correction for raw CO2

As pointed out by Karion et al. (2013), the Picarro G2401 CRDS has a critical orifice (indeed a proportional valve kept always at the same aperture or closed) at the inlet of the cavity, and a proportional valve at the outlet of the cavity and upstream the vacuum pump. Since the cavity pressure is kept at 140 Torr (by controlling the opening of the Outlet Valve), the flow in the critical orifice is supersonic, and therefore, ideally only depends on the CRDS upstream quantities (mainly on the inlet pressure; see Appendix A for more details) and not on the cavity quantities. Therefore, we can assume a linear relationship between the CRDS inlet pressure and the Outlet Valve aperture for small deviations with respect to reference values.

The empirical relation we determined through the inlet pressure sensitivity test mentioned in Sect. 2 leads to the following Outlet-Valve-corrected raw CO2:

$$CO2ovc = CO2raw + 0.04 \cdot (OV - 26468.15)/7700 \qquad (1).$$

CO2ovc is the raw value we use for the CO_2 processing. It is corrected from the inlet pressure sensitivity but not for the H_2O dilution and pressure broadening. According to the knowledge of the authors, this is a new correction not considered previously in the scientific literature. In Appendix A, we provide a plausible physical explanation for this effect, after physically determining the inlet pressure and H_2O dependences of the CRDS flow and physically arguing that the pressure field inside the CRDS cavity is slightly inhomogeneous.

3.2 Raw CH4

We call CH4raw to the raw CH4 multiplied by 1000 (to have ppb units) and use it for the CH4 processing. Note that CH4raw is the wet value not corrected from H2O dilution and pressure broadening.

3.3 Computed raw wet CO

5   The CO value provided by the G2401 CRDS includes the correction due to H2O dilution and pressure broadening. However, what we use for CO processing is the CO raw value (wet) that Picarro calls peak84_spec_wet (*p84sw*), which is *p84* corrected from the H2O and CO2 spectral peak overlapping (interference that changes the zero of *p84*). To compute it, we use the equations that our G2401 employs internally (Rella, private communication):

$$co2\_p14 \ = \ 0.706630873 \cdot p14 \tag{2},$$

10   $$p84sw \ = \ p84 + off + w1 \cdot bh + wc \cdot bh \cdot co2\_p14 + w2 \cdot bh^2 + c1 \cdot co2\_p14 \tag{3},$$

where   *off*=-0.000800885106752,   *w1*=-0.0334069906515,   *wc*=-8.2480775807e-7,   *w2*=0.00633381386844,   and c1=8.87510231866e-6. We call *p84sw'* to *p84sw* multiplied by 1000. That is the raw value we use for the CO processing, i.e., it is the wet value not corrected from H2O dilution and pressure broadening nor converted to ppb units.

4 Calibrations and Response Functions

15   After processing, the measurements we carry out with the CRDS are in the following WMO scales: X2007 for CO2, X2004A for CH4 and X2014A for CO, since we use 4 multi-specie WMO tertiary standards filled (with dried natural air) and calibrated by the WMO CCL (Central Calibration Laboratory) for these gases (https://www.esrl.noaa.gov/gmd/ccl/).

In each cycle of a calibration we use the 4 WMO tertiary standards and 2 target gases that act as unknowns. Each tank is measured continuously during 30 minutes every cycle. From December 2015 to August 2016, each calibration had 5 cycles

20   and a calibration was performed every 3 weeks. From September 2016 till present, each calibration has 2 cycles and a calibration is performed every month. In the first period, we adopted a conservative strategy and after analysing the obtained results in detail we concluded that the second calibration strategy provided accurate-enough results. Note that since there are technicians at the station every day, the regulators of the WMO tertiary standards remain closed between calibrations. This avoid any hypothetical problem of drifting in the standards due to very small leaks or differential diffusion inside the

25   regulators that might propagate till the interior of the standards through the open valves by diffusion during the weeks the standard air remains static inside the regulators. For CO2 and CH4, the last 10 minutes of each gas injection are used. However, for CO, the last 20 minutes are used since CO measurements are noisier (i.e., better signal to noise ratio when incrementing the averaging period) and 10 minutes of stabilization time is enough for CO (numeric details not presented here).

The calibration processing is done using our own Fortran 90 code. For processing a calibration, the code computes the mean raw response for each tank and specie, and then performs a least-square fit to the respective response function detailed below. For CH4 and CO, we use linear response functions:

$$CH4raw = b \cdot CH4 + c \qquad (4), \text{ and}$$

5 $$p84sw' = b \cdot CO + c \qquad (5),$$

where CH4 and CO are the real dry mole fractions (the gas standards are dry) in ppb. For CO2, a quadratic function with raw signal slightly corrected in the outlet valve aperture is used (as described in Sect. 3.1):

$$CO2ovc = a \cdot CO2^2 + b \cdot CO2 + c \qquad (6),$$

where CO2 is the real dry mole fraction in ppm. Since b is always positive (and near 1) and a is always negative and near
10 zero, CO2 is given by this solution of the second-order algebraic Eq. (6):

$$CO2 = \left[-b + \sqrt{b^2 - 4 \cdot a(c - CO2ovc)}\,\right]/(2 \cdot a) \qquad (7).$$

To assess the drift in time of the response function from December 2015 to July 2017, we use the concept of virtual tank of fixed mole fractions (Yver Kwok et al., 2015) and compute the raw values associated to those mole fractions using the response functions obtained in the calibrations. We consider a virtual tank with 400 ppm of CO2, 1850 ppb of CH4 and 100
15 ppb of CO. Moreover, we present here a justification of that procedure and complement it by using the local slope of the response function at the mole fraction of the virtual tank for each specie. In the field of high-accurate atmospheric trace-gas measurements, the calibration fits use to be performed using a limited range in the independent variable that is far from zero (a range around the atmospheric mole fractions of interest). This produces an anticorrelation between the coefficients b and c. The reason is the fact that if b has a positive error (larger slope) then c will have a negative error (smaller Y-intercept) that
20 will increase in absolute value as the distance between the used X-range and zero increases. Therefore, plotting the time series b and c is not the best option for assessing the stability in time of the response function, since part of the variability is due to the anticorrelation and does not correspond with a real variability within the X-range of interest. A more interesting option is to plot the Y-value corresponding to a X-value located within the range of interest instead of c (virtual tank concept) and the local slope at that X-value. Note that for CH4 and CO, which have linear response functions, the local slope
25 does not depend on mole fraction and is equal to the coefficient b.

Figure 1 shows the CRDS raw responses for that virtual tank computed using the response functions obtained in the calibrations. From Figure 1, we obtain the CRDS long-term drift of the raw responses: 0.104 ppm/year for CO2, 2.22 ppb/year for CH4, and 0.544 ppb/year for CO. We define CH4frac=CH4raw/1850 and CO2frac=CO2ovc/400, i.e., they are the raw mole fractions of the virtual tank divided by the real mole fractions. Figure 2 shows a scatter plot of CH4raw versus
30 CO2ovc for the virtual tank. When fitting a linear function, the obtained slope is 20.788 ppb/ppm, which is equal to 4.495 when using the fractional variables, CH4frac and CO2frac.
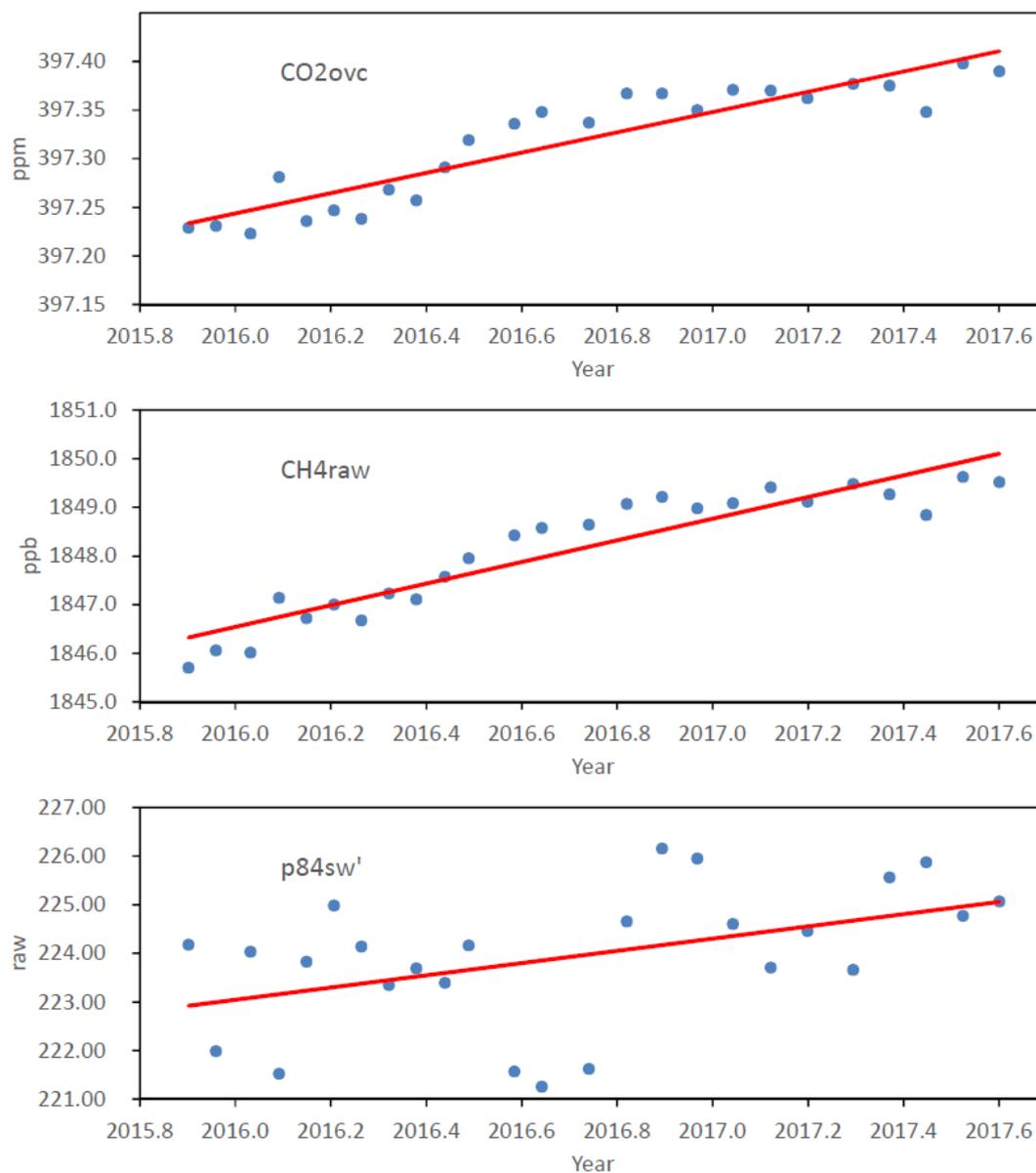
Figure 1: CRDS raw responses (blue dots) for a virtual tank (400 ppm of CO2, 1850 ppb of CH4, and 100 ppb of CO) computed using the response functions obtained in the calibrations. Each red line corresponds to a least-square fitting of the data to a linear function.

Assuming that those drifts are due to drifts in the real pressure and temperature of the cavity and taking into account the fact that the empirical sensitivities (partial derivatives) of the CRDS raw CO2 and CH4 with respect to CP and CT are known

(Yver Kwok et al., 2015), we have determined that our CRDS has a long-term drift of 0.152ºC/Torr and 0.446 Torr/year in the cavity sensors, using the following relations between partial derivatives:

$$\frac{dCH4frac}{dCO2frac} = \left(\frac{\partial CH4frac}{\partial T}\cdot\frac{dT}{dp}+\frac{\partial CH4frac}{\partial p}\right)/\left(\frac{\partial CO2frac}{\partial T}\cdot\frac{dT}{dp}+\frac{\partial CO2frac}{\partial p}\right) \quad (8), \text{ and}$$

$$\frac{dCH4frac}{dt} = \left(\frac{\partial CH4frac}{\partial T}\cdot\frac{dT}{dp}+\frac{\partial CH4frac}{\partial p}\right)\frac{dp}{dt} \quad (9),$$

5   where the partial derivates of the fractional mole fractions with respect to the temperature and pressure have been obtained from Sect. 3.3.6 of Yver Kwok et al. (2015). Note that the use of Eqs. (8) and (9), which provide a quantitative estimation of the drift in temperature and pressure, is a novelty introduced in the present paper.
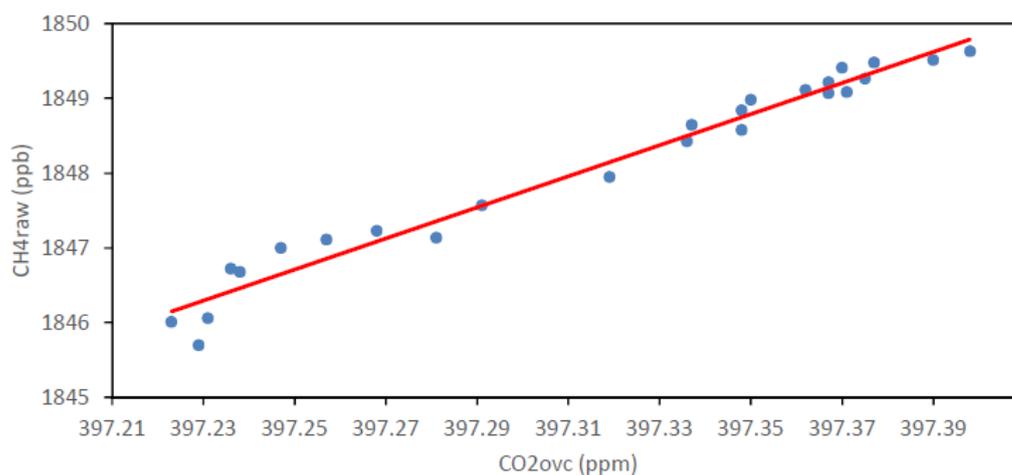
Figure 2: Scatter plot of CH4raw versus CO2raw for the mentioned virtual tank. The red line has been obtained performing a
10 **least-square fitting of the data to a linear function.**

Figure 3 provides additional information about the response functions determined in the calibration. In detail, Fig. 3 provides for each specie the local slope of the response function at the mole fraction of the virtual tank, as well as the quadratic coefficient (*a*) for the CO2 response function.
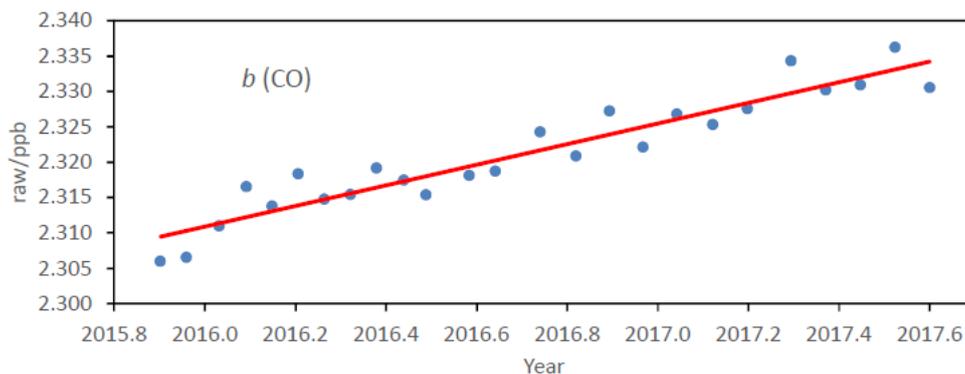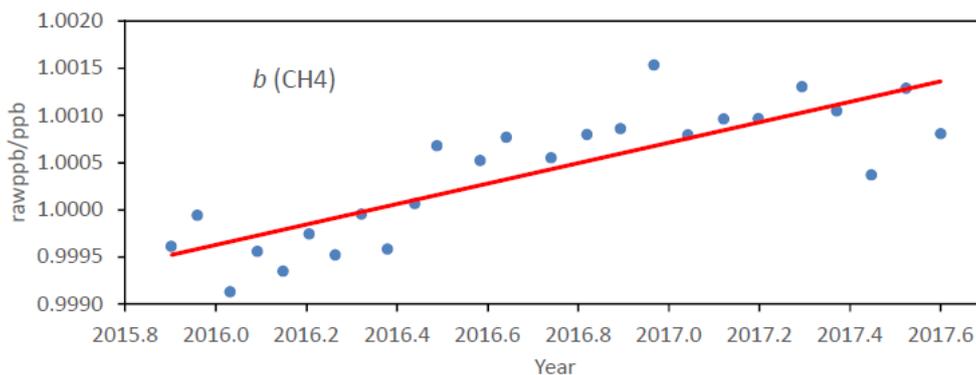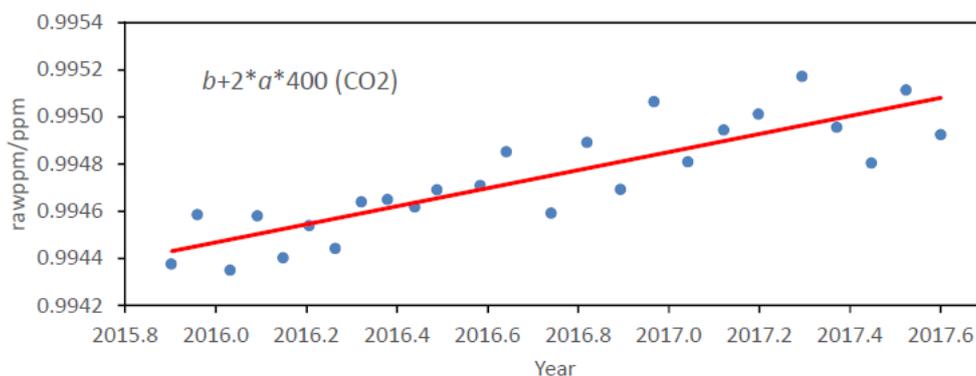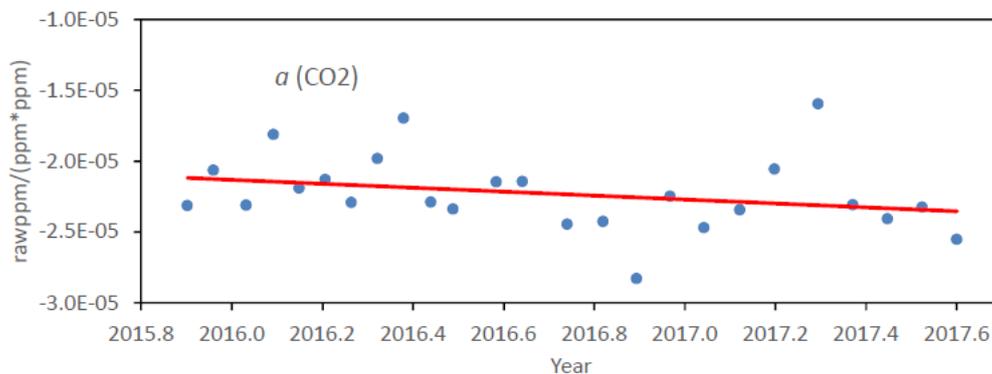
Figure 3: Quadratic coefficient of the CO2 response function (*a*) and local slope of the response function at the mole fraction of the virtual tank, for CO2, CH4 and CO. Note that for CH4 and CO, the local slope does not depend on mole fraction and is equal to the coefficient *b*. The red line corresponds to a least-square fitting of the data to a linear function.

Figure 4 provides for each specie and calibration the RMS residual of the fit and the difference between the assigned mole

5   fraction to a target gas and the mean mole fraction of such target gas. For CO2, the mean RMS residual for all the

calibrations is 0.021 ppm, there is no trend in the associated time series, and the maximum departure in absolute value of a

target gas assignment from the mean for such target gas is 0.026 ppm. Those numbers are quite small compared with the

GAW DQO for CO2, and indicate a good performance of the measurement system for CO2. For CH4, the mean RMS

residual for all the calibrations is 0.09 ppb, there is no trend in the associated time series, and the maximum departure in

10   absolute value of a target gas assignment from the mean for such target gas is 0.18 ppb. As for CO2, those numbers are quite

small compared with the GAW DQO for CH4 and indicate a good performance of the measurement system for CH4.

However, for CO, there is a significant trend in the time series of RMS residuals, which had a value of around 0.1 ppb for the

first calibrations whereas it was around 0.7 ppb for the last ones. Moreover, there are significant downward drifts in all the

time series of target gas assignments, which is a very strange fact since CO standards use to drift upward. All these facts

15   suggest that the IZO CRDS CO WMO tertiary standards might be drifting upward quite significantly at different rates.
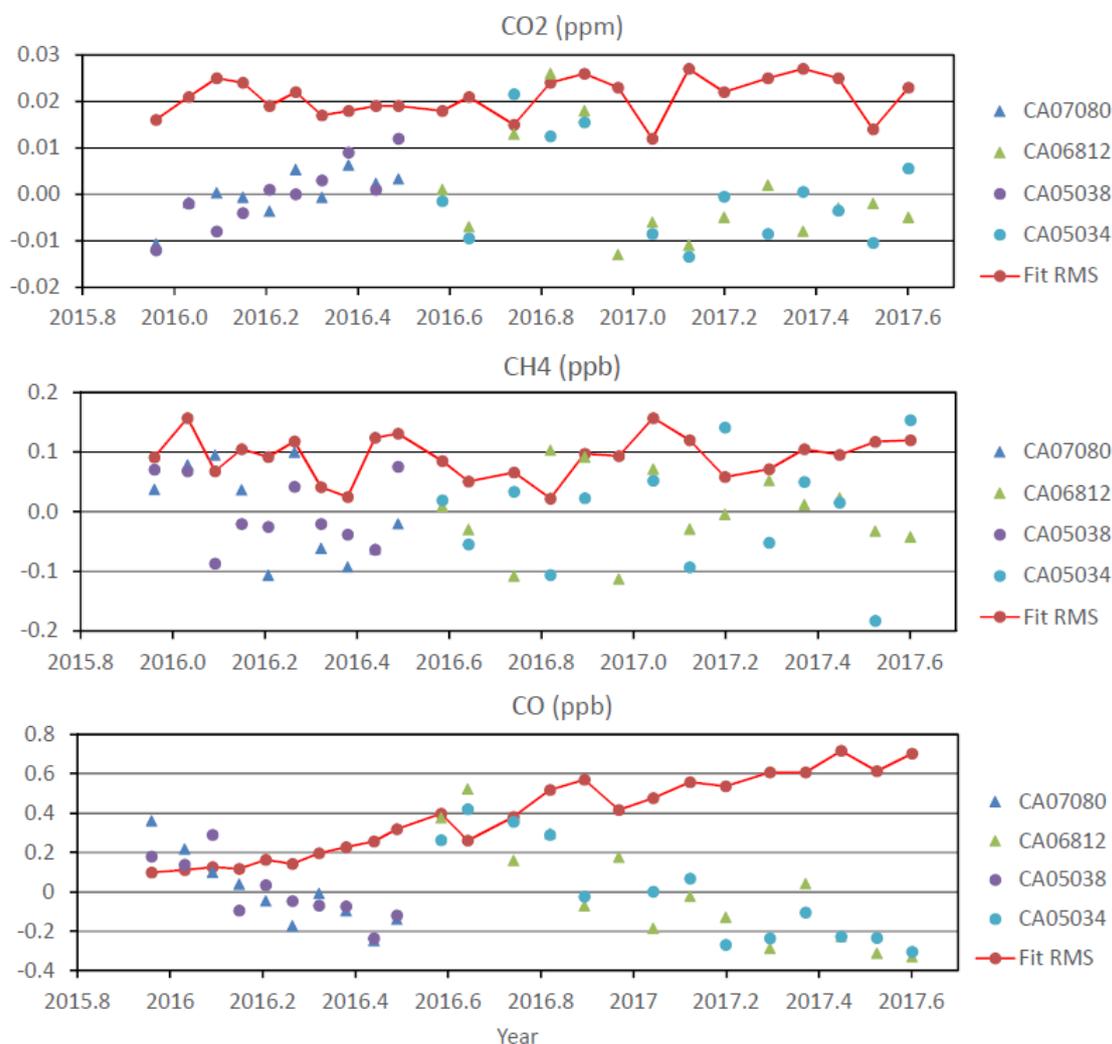
Figure 4: RMS residual of the fit (red dots/line), and difference between the assigned mole fraction to a target gas and the mean mole fraction of such target gas (a different colour is used for each target gas), for each specie and calibration.

5 Water Vapour Correction: water droplet method

5   The natural air contained in the WMO tertiary standards and the target standards is dry. However, ambient air contains water vapour and if it is not completely dried before measurements (as it is done in NDIRs), the dilution and pressure broadening effects due to H2O need to be taken into account and corrected (Chen et al., 2010; Zellweger et al., 2012; Rella et al., 2013, Chen et al., 2013; Karion et al., 2013).

For determining the particular water vapour dilution and pressure broadening corrections for the IZO CRDS G2041, we

10   performed a long water droplet test (around 12 hours) using crushed (to increase the surface/volume ratio) Silica Gel balls

soaked with deionized water contained in a stainless steel filter housing (called MPI/NOAA implementation in Rella et al., 2013), as Fig. 5 shows. The dry natural air coming from a standard flowed continuously during around 12 hours through the wet Silica Gel before being measured in the CRDS. Figure 6 shows the evolution in time of the h2o_reported (*hr*) in pph (parts per hundred in mole fraction) determined by the CRDS.

Figure 5: Experimental setup used for the water droplet test performed to the IZO CRDS G2401.
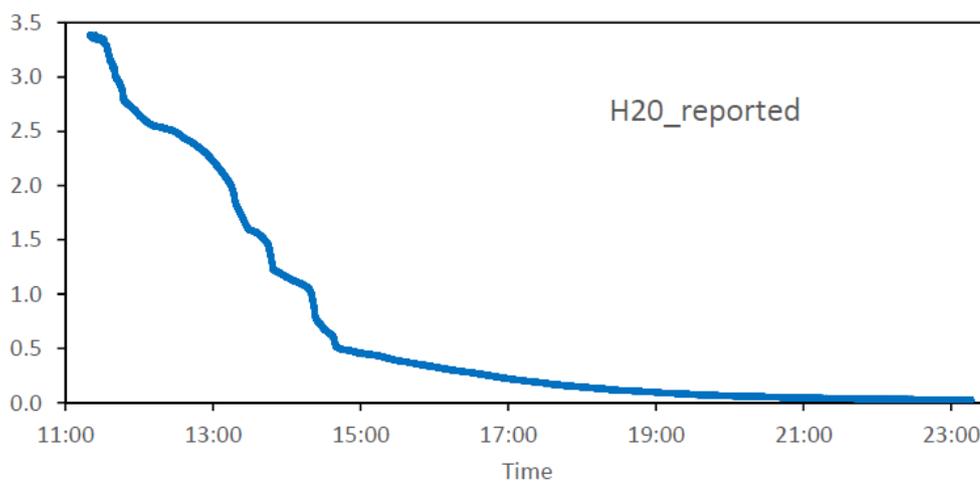
Figure 6: Evolution in time of the h2o_reported (pph) determined by the CRDS.

For CO2 and CH4, we use these empirical correction equations for the H2O dilution and pressure broadening effects (Chen et al., 2010):

$$CO2ovc\_wet = CO2ovc\_dry \cdot (1 + d \cdot hr + e \cdot hr^2) \qquad (10),$$

$$CH4raw\_wet = CH4raw\_dry \cdot (1 + d \cdot hr + e \cdot hr^2) \qquad (11),$$

where CO2ovc_dry, CH4raw_dry, d and e (different in each equation) are determining by least-square fitting to test results. Since the experiment is very long, before performing the least-square fit, we aggregate data computing 100-data means. That

5 corresponds approximately to a 59-second mean, since there are 1.7 data per second. For CO2, we obtained coefficients d and e very close to those reported by Chen et al. (2010). Thus, we decided to use their coefficients, d = -0.012 pph^{-1} and e = -0.000267 pph^{-2}. Figure 7 shows CH4raw versus hr during the experiment and the least-square fitted curve, being the coefficient obtained for CH4: d = -0.009974 pph^{-1} and e = -0.0001757 pph^{-2}.
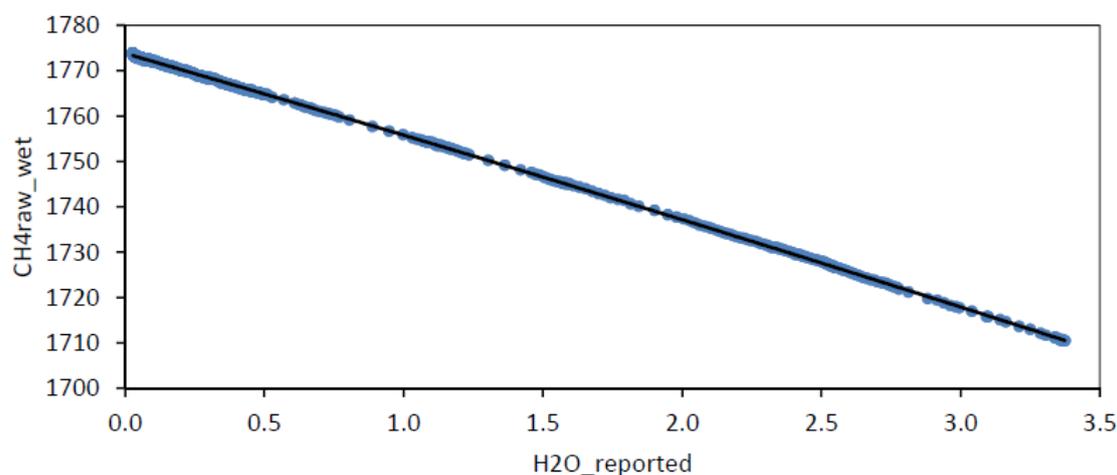
Figure 7: CH4raw versus *hr* during the water droplet experiment (in blue) and the least-square fitted curve (in black).

For CO, we rely on the H2O dilution and pressure broadening correction determined by Rella (2010), as other authors have done (Chen et al., 2013; Laurent, private communication), and determine an improvement in the correction for the CO peak

15 interference (zero error or spectral-baseline correction) due to the nearby H2O peak, respect to the factory values. To this end, we use a simple and accurate novel method. We consider the equation:

$$p84sw' + A \cdot bh + B \cdot bh^2 + C \cdot bh^3 = p84sd' \cdot (1 + d \cdot bh + e \cdot bh^2) \qquad (12),$$

which is equivalent to Eqs. (10) and (11) except for the cubic polynomial on the left-hand side that accounts for the mentioned CO spectral-baseline correction. We use d = -0.01287 and e = -0.0005365 (Rella, 2010), and *p84sd'*, *A*, *B*, and *C*

20 are determined by least-square fitting of the experimental data to the cubic equation:

$$p84sw' = p84sd' + (d \cdot p84sd' - A) \cdot bh + (e \cdot p84sd' - B) \cdot bh^2 - C \cdot bh^3 \qquad (13),$$

obtained rearranging Eq. (12). The instantaneous CRDS CO signal is quite noisy, but the noise is significantly reduced by using 4000-data running means (39.2-minute approximately) without compromising the accuracy of the data. Note that least-square fits are very sensitive to outliers, and the fit will be more accurate if the 4000-data running mean is performed

previously. As far as the authors know, this is a novel method not done before. It is important to have a very accurate H_2O correction, since in spite of the fact the instantaneous CRDS CO values are quite noisy, such noise decreases significantly when performing successively 30-second, 1-hour, 12-hour means, whereas the hypothetical error in the H_2O correction remains constant behaving as a bias. After performing the 4000-data running means, we aggregate data computing 100-data means as for CO_2 and CH4. Figure 8 shows *p84sw'* versus *bh* during the experiment and the least-square fitted curve corresponding to Eq. (13). After determining the coefficients of that cubic polynomial, we solve for the unknown constants in Eq. (12): A = -5.287565 raw/pph^{-1}, B = 5.283987 raw/pph^{-2}, and C = -1.120169 raw/pph^{-3}. The absolute value of A is much smaller than 1000*|w1|, which appears in Eq. (3). This means A is indeed a relatively small correction. On the contrary, B and C are very significant corrections comparing with their respective terms in Eq. (3), in which there is not cubic term.
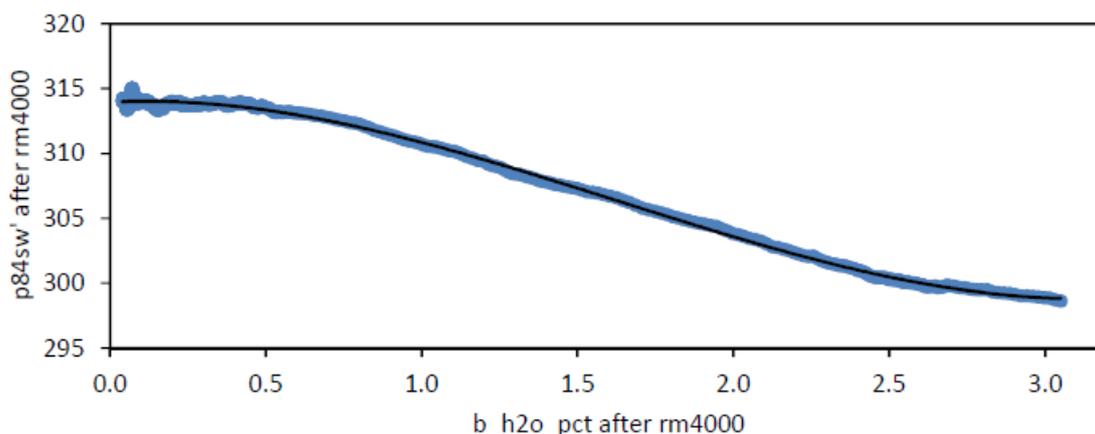
Figure 8: *p84sw'* versus *bh* during the water droplet experiment (blue dots), both after performing a 4000-data running mean, and the least-square fitted curve corresponding to Eq. (13) in black.

6 Ambient Measurements

Figure 9 shows the ambient air/gas standard plumbing configuration operative since 28 November 2016. Before that date, there were no "Dedicated inlet", no drying (no cooled flasks), no solenoid nor needle valves, and ambient air entered through the MPV. Operative ambient air measurements started on 27 November 2015. Target gas measurements started on 18 December 2015 with a 7-hour cycle (3 hours of ambient, 30 minutes of target 1, 3 hours of ambient, and 30 minutes of target 2) to monitor better the behaviour of the CRDS, which became a 21-hour cycle after 24 June 2016. With the new plumbing configuration, ambient air is alternatively sampled from the two inlet lines within the 21-hour cycle (15 hours of ambient from the dedicated inlet and 5 hours of ambient from the general inlet). Since the cooler bath temperature is -40 °C, there is

no complete drying. Therefore, it has been necessary to apply the H2O water vapour correction for the full measurement period.
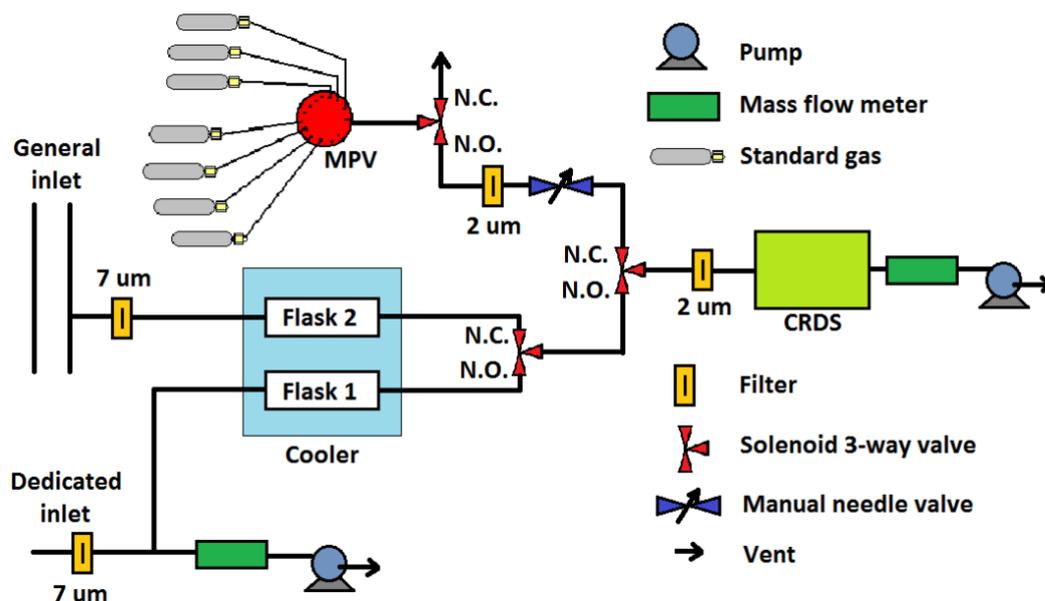
Figure 9: Ambient air/gas standard plumbing configuration operative since 28 Nov 2016.

6.1 Ambient Air Measurement Processing

After performing the pre-processing detailed in Sect. 3, we apply an additional filtering to the 30-second means. For not discarding a pre-processed 30-second mean: 1) the mean values of the following variables need to be within the indicated ranges: *CP*: 140 +- 0.035 Torr, *CT*: 45 +- 0.02 ℃, and OV: 20000-40000; 2) it needs to exit a calibration before and after the ambient mean considered, separated in time less than 180 days between them, as in ICOS (Hazan et al.,2016).

Then, we apply the following processing scheme. Firstly, we apply water vapour correction: a) using Eqs. (10) and (11) we compute CO2ovc_dry and CH4raw_dry from CO2ovc_wet, CH4raw_wet and *hr* (i.e., dilution and pressure broadening effect correction); b) using Eq. (12) we compute p84sd' from p84sw' and *bh* (i.e., refinement of the interference correction as well as dilution and pressure broadening effect correction). Secondly, we apply the calibration curves interpolated linearly in time: a) for CO2, we employ Eq. (7) using CO2ovc_dry where it says CO2ovc; b) for CH4, we employ Eq. (4) using CH4raw_dry where it says CH4raw; and c) for CO, we employ Eq. (5) using p84sd' where it says p84sw'. Finally, we proceed to discard data due to the stabilization time: 10 minutes for ambient measurements, and 20 minutes for target and calibration gas injections.

6.2 Target Gas Injections

Table 3 summarizes the statistics for the target gas injections (30-second-mean assignments), whereas Fig. 10 shows the time series of mole fraction assignments for one of the target gases. The results are good. Note that 30-second is a too short time for CO, and it is necessary to consider longer averages for reducing noise. The ambient processing scheme described in Sect.

5   6.1 is also used to assign mole fractions to the target and calibration gas injections, and it is checked that the water vapour correction for them is smaller than 0.01 ppm for CO2, and 0.1 ppb for CH4 and CO.
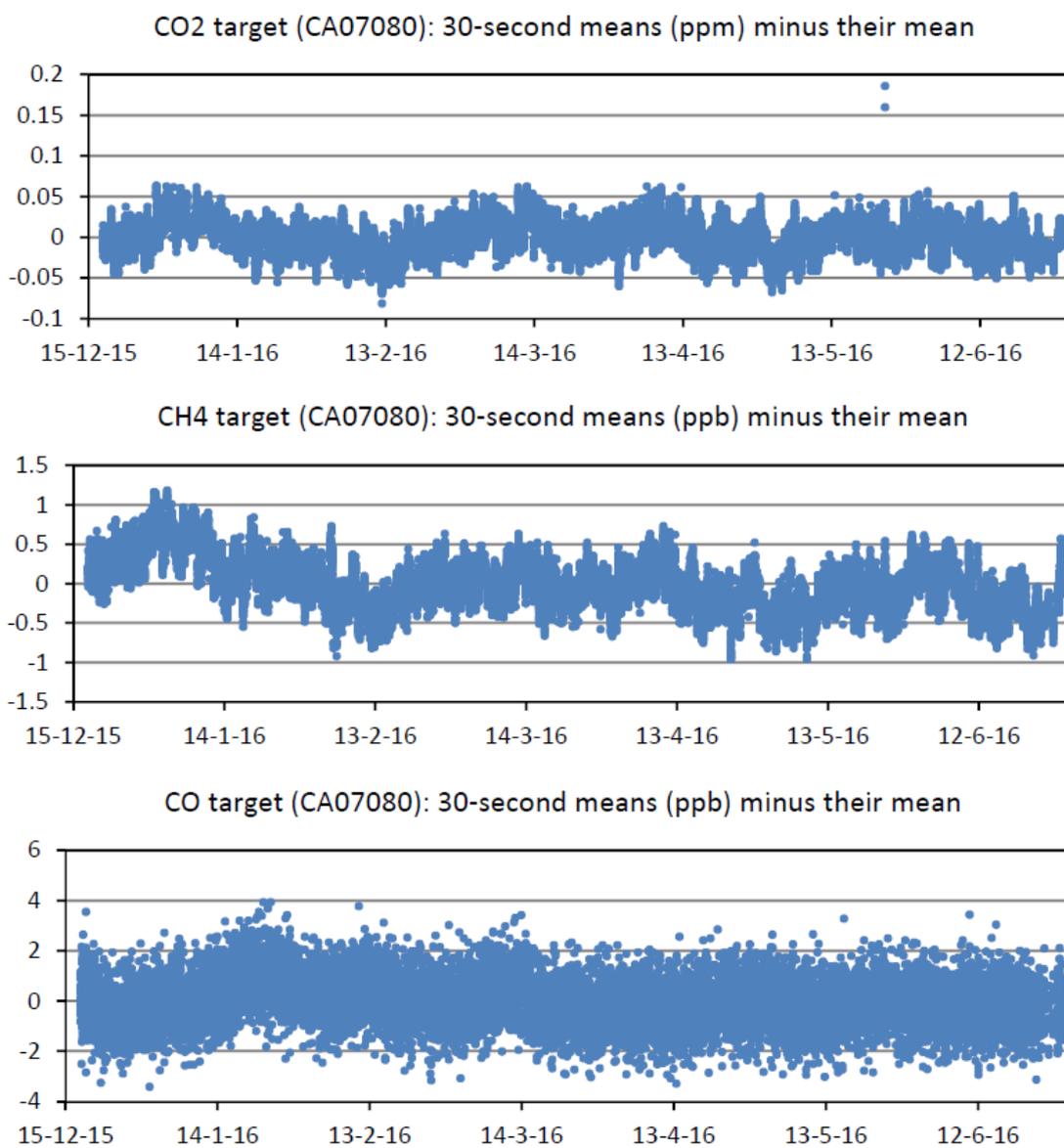
Figure 10: Time series of mole fraction assignments for one of the target gases.

Tank/months	CO2 (ppm)	Std.dev.	CH4 (ppb)	Std.dev.	CO (ppb)	Std.dev.
CA07080/ 7m	381.96	0.020	1825.43	0.32	148.60	0.97
CA05038/ 7m	368.85	0.020	1777.04	0.33	93.56	0.99
CA06812/ 13m	372.48	0.020	1784.80	0.27	142.04	1.01
CA05034/ 13m	363.71	0.020	1775.89	0.27	139.11	0.98

Table 3. Statistics for the target gas injections (30-second-mean assignments): mean and standard deviation (Std.dev.)
5   **for the different species.**

6.3 Comparison with other continuous measurements carried out at Izaña

In this subsection, we compare the CRDS IZO ambient daily-nighttime (from 20:00 UTC of the previous day till 8:00 of the considered day) means with the co-located hourly means from the IZO Li7000 NDIR for CO2 (Gomez-Pelaez et al., 2011; Gomez-Pelaez et al., 2014; Gomez-Pelaez et al., 2016), IZO Varian GC-FID for CH4 (Gomez-Pelaez et al., 2011; Gomez-
10   Pelaez et al., 2012; Gomez-Pelaez et al., 2016), and IZO RGA-3 GC-RGD for CO (Gomez-Pelaez et al., 2013; Gomez-Pelaez et al., 2016), all of them in the scales already indicated in Sect. 4. We use daily-nighttime means for the comparison because: 1) as mentioned in the introduction, IZO has background conditions during nighttime; and 2) when using 12-hour averages, we improve the signal to noise ratio and remove any hypothetical dependence on the used IZO general inlet due to small inhomogeneities in space and time of the mole fraction fields in space. Note that the data for 2017 are still not final.
15   Figure 11 shows the time series of daily-nighttime CRDS measurements, whereas Table 4 shows the monthly-mean differences between the daily-nighttime CRDS measurements and those for the rest of the mentioned IZO instruments. As Table 4 shows, for CO2 and CH4 the differences between the instruments are within the GAW compatibility objectives (0.1 ppm for CO2 and 2 ppb for CH4), except for 4 months for the former and 3 months for the later (coincident with those for CO2). However, for CO the difference between the instruments is larger than 2 ppb after March 2016. The WMO tertiary
20   standards used in the RGA-3 have been calibrated two times by the WMO CCL and the inferred drifts were considered significant, extrapolated forward in time, and taken into account in the RGA-3 data processing. These results seem to support the hypothesis that the observed negative differences are explained by the fact that the CRDS laboratory standards (WMO tertiaries) might be drifting up significantly for CO (see Sect. 4). Maybe, there could be also a small contribution from WMO CO Primaries of the X2014A scale drifting less than initially computed by CCL, which is a recent suspicion of the CCL that
25   needs to be checked during the next two years (Crotwell, communication during GGMT-2017).
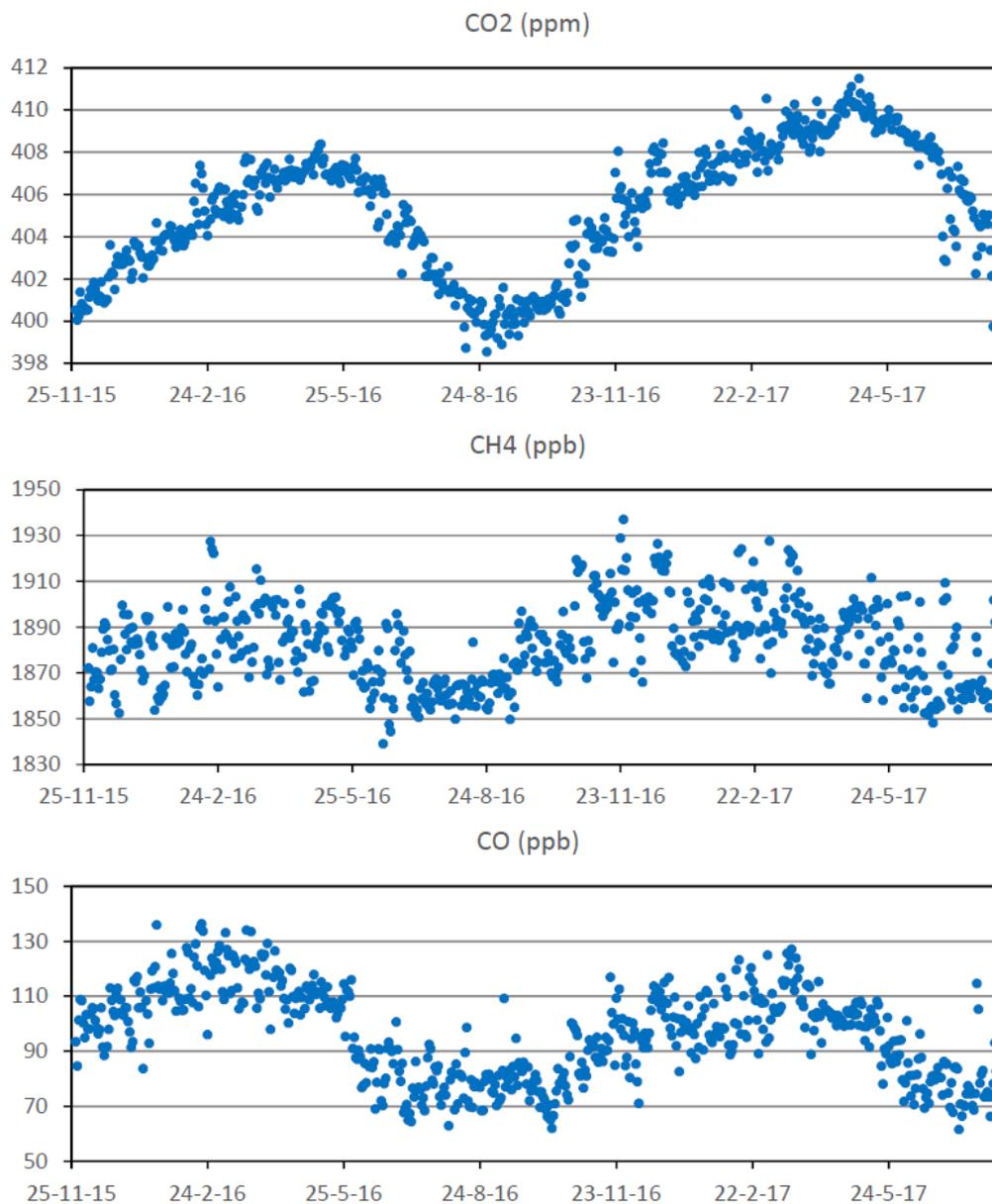
Figure 11: Time series of daily-nighttime CRDS measurements (CO2, CH4 and CO).

Year	Month	CO2 CRDS - CO2 Li7000 (ppm)	CH4 CRDS - CH4 VarianFID (ppb)	CO CRDS - CO RGA3 (ppb)
2015	2017	**-0.07**	**1.2**	**-2.8**
2015	11	-0.08	1.6	-0.4
2015	12	-0.04	0.9	-1.1

2016	1	-0.03	1.0	-1.3
2016	2	-0.08	1.0	-1.8
2016	3	-0.07	0.3	-2.4
2016	4	-0.06	-0.1	-2.7
2016	5	-0.02	0.2	-2.9
2016	6	-0.03	0.9	-3.0
2016	7	0.00	1.1	-3.2
2016	8	0.05	1.9	-2.9
2016	9	-0.10	2.0	-3.1
2016	10	-0.12	3.3	-4.1
2016	11	-0.15	3.1	-3.0
2016	12	-0.07	0.5	-3.7
2017	1	-0.09	1.1	-3.0
2017	2	-0.14	2.1	-3.3
2017	3	-0.11	0.5	-3.6
2017	4	-0.08	0.4	-2.7
2017	5	---	0.3	-3.4

Table 4: Monthly-mean differences between the daily-nighttime CRDS measurements and those for the rest of the mentioned IZO instruments (Li7000 NDIR for CO2, Varian GC-FID for CH4, and RGA-3 GC-RGD for CO).

.

7 Preliminary independent assessment on the drift rates of the CRDS CO standards

5   Some few facts presented in Sect. 4 and Sect 6.3 seem to indicate the CRDS CO WMO tertiary standards might be drifting significantly. These standards have been calibrated only once by CCL: in August-September 2015. In order to perform a preliminary independent assessment on the drift rates of the CRDS CO standards, we have proceeded as follows. As mentioned in Sect 6.3, the WMO tertiary standards used in the RGA-3 have been calibrated twice (9 years distant) by the WMO CO CCL and the inferred drifts were considered significant and extrapolated forward in time. We have performed a 4-

10   cycle calibration in the CRDS for comparing the CRDS standards (CB11240, CB11389, CB11393, and CB11340) and the RGA-3 standards (CA06968, CA06768, CA06988, CA06946, and CA06978). The first step has been assigning CO2 and CH4 mole fractions to the RGA-3 standards using the calibration curves obtained using the CRDS standards. The second step has been assigning CO mole fractions to the CRDS standards using the calibration curve obtained using the RGA-3 standards, whose fit RMS residual is 0.4 ppb. In the third step, we determined the drift rate of each CRDS standards using

15   the CCL assignment done in 2015 and the present assignment (done on 4 October 2017), which is indirectly traceable to the

WMO primaries. The standard CB11240 is the only one with a significant drift rate, 1.21 ppb/year, having 195.87 ppb at present. The other three standards have all positive drift rates, being the maximum 0.17 ppb/year. We have performed the exercise of reprocessing all the CRDS calibrations taking into account the drift rates determined for the four CRDS standards (even those not statistically significant), as show in Fig. 12. Comparing Fig. 12 with Fig. 4c, we see now there is no trend in the RMS residual from the calibration fit and the downward drift of the target gases is significantly smaller. However, when reprocessing the CRDS ambient CO time series, the maximum improvement in the CRDS minus RGA-3 monthly difference time series is 0.3 ppb for some periods, remaining unchanged the global mean difference for the full period. Therefore, we infer the performance of the calibrations improves largely when taking into account the quite significant drift in the standard CB11240, but the CRDS versus RGA-3 ambient differences remain almost unchanged.
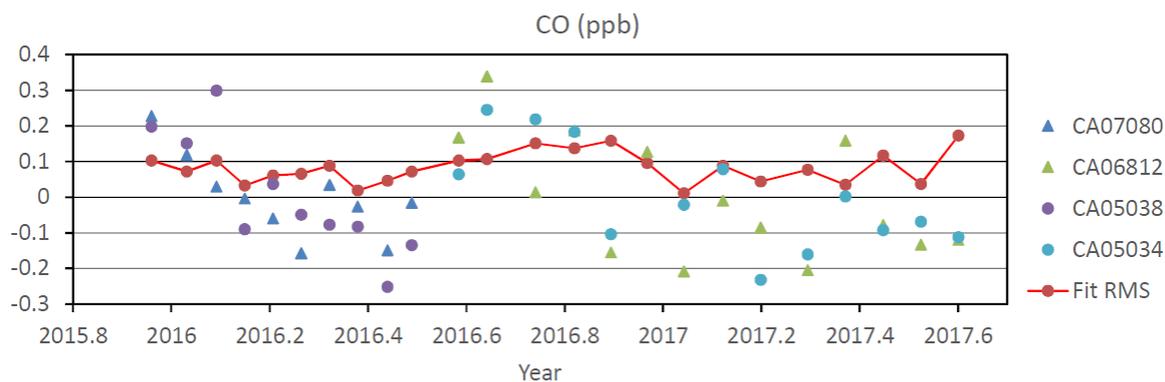
Figure 12: RMS residual of the fit (red dots/line), and difference between the assigned mole fraction to a target gas and the mean mole fraction of such target gas (a different colour is used for each target gas), for each specie and calibration, after taking into account the drift rates of the CRDS standards.

8 Summary and Conclusions

- At the end of 2015, a CO2/CH4/CO CRDS was installed at the Izaña Global GAW station to improve the Izaña GHG GAW measurement programme and guarantee its long-term maintenance. The results of the CRDS acceptance tests were good. However, a correction for CO2 that takes into account the inlet pressure had to be incorporated in order to achieve a RMS residual of around 0.02 ppm, which is the value we obtain with the IZO NDIR based measurements systems. For CO, our data processing is based on the raw spectral peak data instead of on the raw CO provided by the instrument.

- We use linear response functions for CH4 and CO, and a quadratic response function for CO2. The CRDS long-term drift of the raw responses is: 0.104 ppm/year for CO2, 2.22 ppb/year for CH4, and 0.544 ppb/year for CO. Assuming that those drifts are due to drifts in the real pressure and temperature of the cavity, we have determined

that our CRDS has a long-term drift of 0.152ºC/Torr and 0.446 Torr/year in the cavity sensors using relations between partial derivatives. We show also the evolution in time of the response-function local slopes at the mole fractions of the virtual tank, as well as the RMS residual in the calibration fits, which has no significant trend except for CO.

- The time series of target gas assignments during calibrations are also shown, which again indicate a good behaviour for CO_2 and CH_4, but a downward drift for CO. Those facts seem to point out the CRDS CO WMO tertiary standards are probably drifting significantly in spite of the fact they have been only used during two years. Using an independent set of CO laboratory standards whose drift rates have been determined by the CO CCL, we conclude that one of the CRDS standards is drifting quite significantly (1.21 ppb/year). The performance in the calibrations improves when taking that drift into account.

- The results of the long water-droplet test (12 hours) have been presented and used for the H_2O water vapor correction. The determination of the H_2O correction for CO presents two novelties: use of the raw spectral peak data and use of a running mean to smooth random noise before performing the least square fit.

- We have presented the ambient measurement scheme and its data processing. Target gas injections show very small standard deviations except for CO. The agreement with other IZO in situ continuous measurements is good most of the time for CO_2 and CH_4, but for CO is just outside the GAW 2-ppb objective. It seems the disagreement is not produced by the drifts in the CRDS CO WMO tertiary standards. The mean differences for the full period are: -0.07 ppm for CO_2, 1.2 ppb for CH_4, and -2.8 ppb for CO.

- We have physically determined and discussed the origin of the inlet pressure and H_2O dependences of the CRDS flow, and pointed out the existence of flow-rate-dependent small spatial inhomogeneities in the pressure and temperature fields inside the cavity. We have shown that the slightly-depleted-in-pressure regions inside the CRDS cavity in the neighbourhood of the inlet and outlet pipes due to the cross-section change, are probably the cause of the slight CO_2 correction associated to the mass flow rate we have empirically obtained. We suggest performing a gas dynamic numerical simulation of the pressure and temperature fields inside the CRDS cavity for different flow rates. This could help to improve the spectral forward model used by the CRDS and also to take into account more accurately the impact of the flow rate on the measurements. On the other hand, the use of conical adapters for connecting the pipes to the CRDS cavity might keep the pressure gradients associated to the cross-section changes out of the laser path.

Code availability. The Fortran 90 codes developed in this work could be made available to other researchers under a cooperative agreement with the Izaña Atmospheric Research Centre (AEMET). However, a very limited support on their use could be provided.

Data availability. The data presented in this paper is available under request. If the supplied data is intended to be used in a
5 scientific article, co-authorship should be offered to data providers.

Appendix A. A note concerning the inlet pressure and H2O dependences of the CRDS flow and the spatial inhomogeneity of the pressure field inside the cavity

A choked flow is a flow through a critical orifice in which the following condition holds for the inlet to outlet pressure ratio (Van den Bosch & Duijm, 2005):

10 $$\frac{p_i}{p_o} \geq \left(\frac{\gamma+1}{2}\right)^{\gamma/(\gamma-1)} \qquad \text{(A1)},$$

where p_i is the inlet pressure, p_o is the outlet pressure, and γ is the ratio of specific heats (c_p/c_v) for the considered gas. For dry air, γ is equal to 1.4 and the right-hand side of Eq. (A1) is equal to 1.893. In a choked flow, the speed is supersonic just downstream the orifice and the flow rate does not depend on the downstream quantities (because "information" cannot propagate faster than sound). Since the minimal recommended inlet pressure for the CRDS G2401 is 0.4 bar and the cavity
15 pressure is 0.167 bar (140 Torr), the flow in the inlet critical orifice is choked. This is the reason by which the flow through the CRDS cavity depends only on upstream quantities (mainly the inlet pressure, as indicated in Sect 3.1), except for Flight-ready models, which have the critical orifice at the outlet of the CRDS cavity, and therefore, the inlet pressure for the orifice is the cavity pressure, which is kept constant.

The theoretical equation relating the standard volumetric flow (F) with the inlet quantities for a choked flow is (Van den
20 Bosch & Duijm, 2005):

$$F = C_d \cdot A \cdot p_i \cdot \frac{T_s}{p_s} \cdot \left[\frac{\gamma \cdot R}{T_i} \cdot \left(\frac{2}{\gamma+1}\right)^{(\gamma+1)/(\gamma-1)}\right]^{1/2} \qquad \text{(A2)},$$

where T_s and p_s are the standard temperature (273.15 K) and pressure (1.01325 bar) respectively, T_i is the inlet temperature, R is the gas constant, C_d is the discharge coefficient (dimensionless) and A is the hole cross-sectional area. Equation (A2) shows that the standard volumetric flow is proportional to the inlet pressure and inversely proportional to the square root of
25 the inlet (absolute) temperature. However, there is also a small dependence on the water vapour mole fraction through the ratio of specific heats and the gas constant, which depend slightly on the H2O mole fraction as follows:

$$\frac{1}{R} = \frac{1-r}{R_d} + \frac{r}{R_{H2O}} \qquad \text{(A3)},$$

where r is the H2O mole fraction in mol/mol, R_d is the gas constant for dry air, and R_{H2O} is the gas constant for H2O;

$$\gamma = \frac{1.4+0.4\cdot r}{1+0.4\cdot r} \qquad \text{(A4)}.$$

In order to estimate the relative impact of water vapour changes on the standard volumetric flow, we need to know approximately the values of C_d and A. To this end, we use the approximate fact: when p_i is 0.7 bar, F is 150 scc/min, and obtain using Eq. (A2) that the product of C_d and A is equal to 1.955e-8 m². Figure A1 shows F and its derivative (with respect to r) as functions of r, for $p_i = 0.7$ bar and $T_i = 293$ K, showing that the relative impact of r on F is small and the

5   derivative is quite constant for the considered r range (0.00-0.05).
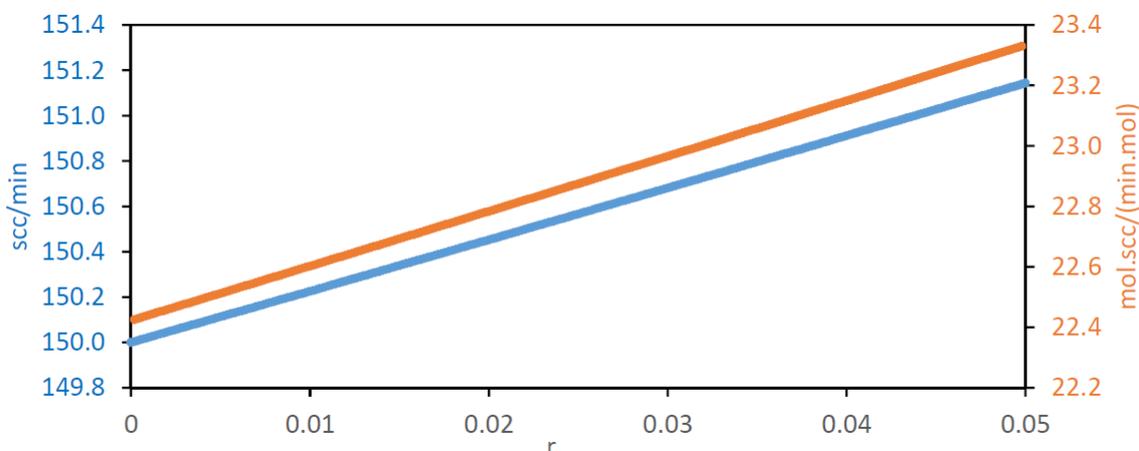
Figure A1: Standard volumetric flow (F) on the left Y-axis and its derivative with respect to r (H2O mole fraction in mol/mol) on the right Y-axis, for $p_i = 0.7$ bar and $T_i = 293$ K.

10   When there is a stationary air flow through an instrument, the pressure field changes spatially mainly due to two reasons (Bernoulli equation): 1) longitudinal decrease of the pressure due to viscosity, and 2) changes in the cross-section along the pipe, which require flow acceleration (provided by a longitudinal pressure gradient) when the cross-section decreases and flow deceleration when the cross-section increases (e.g., Venturi effect). The structure of the optical cavity of the CRDS G2401 is shown in Fig. 1 of Crosson (2008). The plane defined by the three mirrors inside the cavity is horizontal (parallel to

15   the surface of the Earth when the instrument is set on its feet on a bench). The inlet and outlet cavity ports are on the top of the cavity. The pressure sensor is on a third port located on the top of the cavity, at the approximate centre (Rella, private communication). Applying considerations of fluid dynamics, we infer the following facts. First, along the sense of flow inside the cavity, there needs to be a very small decrease in pressure in order to be able to balance the resistance to flow due to viscosity, and that decrease will be larger as the mass flow rate is increased. Since the pressure sensor is located in the

20   middle of the cavity, the mean pressure will be monitored. A parcel of fluid flowing along the cavity will expand very slightly (due to the decrease in pressure that the Lagrangian parcel "feels"), and therefore, the temperature will tend to slightly decrease adiabatically in all the points of the volume whereas the heat to compensate it comes from the surface of the cavity. That is, necessarily there needs to be also a small inhomogeneity in the temperature field inside the cavity, and this inhomogeneity depends on the flow rate. The hypothetical net effect on the measurements is difficult to assess a priori

without performing a gas dynamics numerical simulation. Second, when a fluid parcel leaves the inlet pipe and enters into the cavity, it feels a large change in the cross-section of the solid material that contents the flow. Therefore, there needs to be a portion of cavity near the inlet with pression increasing in the flow sense to decrease and accommodate the velocity of the fluid. That is, in the cavity near the inlet, there is a pressure smaller than in the rest of the cavity. Moreover, the opposite

5   process happens in the cavity near the outlet: the fluid needs to be accelerated, and therefore, there needs to be a portion of cavity near the outlet with pression decreasing in the flow sense. That is, in the cavity near the outlet, there is a smaller pressure than in the rest of the cavity, as happens near the inlet, and this decrease is larger when the mass flow rate is increased. If any portion of those two regions is crosses by the laser path, the perturbation this produces in the measurements agrees in sign with Eq. (1). Therefore, this might be the explanation of the empirically observed effect described in Sect. 3.1.

10   All the effects pointed out in this section, which are new in the GHG measurement literature according to the knowledge of the authors, might modify the conclusions of Reum et al. (2017).

Appendix B. Some additional novelties in the Izaña GHG instrumentation since GGMT-2015

As mentioned in the talk the main author of the present paper gave at GGMT-2017, we have introduced the following

15   improvements in the dedicated inlet lines of the IZO GHG measurement systems: 1) backpressure regulators for the vents located downstream the pumps, and rotameters for those vents; 2) needle valves in low flow vents installed downstream the cryotraps; 3) glass flask cryotraps with Ultra-Torr connections; and 4) hermetic plugs for unused ports of the rotary Valco valves.

We have prepared two CO_2 laboratory standards of 418.7 ppm for the Izaña NDIRs Li7000 and Li6252 (using two cylinders

20   that have proved to be very stable in previous uses as CO_2 working standards), and calibrated them against our CRDS WMO laboratory standards using the G2401 CRDS.

We have reprocessed the Izaña time series of CH_4 and CO in the scales X2004A and X2014A, respectively, taking into account also the drift of the five WMO laboratory standards used in the Izaña RGA-3.

25   **Author contribution**. A.J. Gomez-Pelaez designed the measurement system, measurement scheme, and response functions, made the CRDS acceptance tests, configured the CRDS, performed the H2O droplet tests, made the Fortran 90 codes, analysed the data, made the study of Appendix A, wrote the manuscript and made the plots. R. Ramos installed the measurement system, helped in the routine operation of the system, and revised the manuscript. E. Cuevas was the PI of the financed R+D infrastructure project by which the CRDS equipment could be purchased and installed at IZO, and revised in

30   detail the manuscript. V. Gomez-Trueba performed the routine calibrations. E. Reyes provided support configuring the CRDS computer, prepared the external media necessary to perform daily copies of the acquired data, and revised the manuscript.

Competing interests. The authors declare that they have no conflict of interest.

Acknowledgements. The acquisition of the instrument was largely financed by European ERDF funds through the Spanish
5   R+D infrastructure project AEDM15-BE-3319 of the Spanish "Ministerio de Economía, Industria y Competitividad". This
study was developed within the Global Atmospheric Watch (GAW) Programme at the Izaña Atmospheric Research Centre,
financed by AEMET. We thank Chris Rella (Picarro, Inc., USA), Christoph Zellweger (EMPA, Switzerland), and Olivier
Laurent (ICOS ATC/ LSCE, France) for providing information of great interest about the Picarro G2401 CRDS, and to the
Izaña observatory staff.

10   **References**

Chen, H., Winderlich, J., Gerbig, C., Hoefer, A., Rella, C. W., Crosson, E. R., Van Pelt, A. D., Steinbach, J., Kolle, O.,
Beck, V., Daube, B. C., Gottlieb, E. W., Chow, V. Y., Santoni, G. W., and Wofsy, S. C.: High-accuracy continuous airborne
measurements of greenhouse gases (CO2 and CH4) using the cavity ringdown spectroscopy (CRDS) technique, Atmos.
Meas. Tech., 3, 375–386, doi:10.5194/amt-3-375-2010, 2010.
15   Chen, H., Karion, A., Rella, C. W., Winderlich, J., Gerbig, C., Filges, A., Newberger, T., Sweeney, C., and Tans, P. P.:
Accurate measurements of carbon monoxide in humid air using the cavity ring-down spectroscopy (CRDS) technique,
Atmos. Meas. Tech., 6, 1031-1040, https://doi.org/10.5194/amt-6-1031-2013, 2013.
Chevallier, F., Ciais, P., Conway, T. J., Aalto, T., Anderson, B. E., Bousquet, P., Brunke, E. G., Ciattaglia, L., Esaki, Y.,
Frohlich, M., Gomez, A., Gomez-Pelaez, A. J., Haszpra, L., Krummel, P. B., Langenfelds, R. L., Leuenberger, M., Machida,
20   T., Maignan, F., Matsueda, H., Morgui, J. A., Mukai, H., Nakazawa, T., Peylin, P., Ramonet, M., Rivier, L., Sawa, Y.,
Schmidt, M., Steele, L. P., Vay, S. A., Vermeulen, A. T., Wofsy, S., and Worthy, D.: CO2 surface fluxes at grid point scale
estimated from a global 21 year reanalysis of atmospheric measurements, J. Geophys. Res., 115, D21307, doi:
10.1029/2010JD013887, 2010.
Crosson, E. R.: A cavity ring-down analyzer for measuring atmospheric levels of methane, carbon dioxide, and water vapor,
25   Appl. Phys. B-Lasers O., 92, 403–408, 2008.
Cuevas, E., González, Y., Rodríguez, S., Guerra, J. C., Gómez-Peláez, A. J., Alonso-Pérez, S., Bustos, J., and Milford, C.:
Assessment of atmospheric processes driving ozone variations in the subtropical North Atlantic free troposphere, Atmos.
Chem. Phys., 13, 1973-1998, doi:10.5194/acp-13-1973-2013, 2013.
Cuevas, E., Milford, C., Bustos, J. J., del Campo-Hernández, R., García, O. E., García, R. D., Gómez-Peláez, A. J., Ramos,
30   R., Redondas, A., Reyes, E., Rodríguez, S., Romero-Campos, P. M., Schneider, M., Belmonte, J., Gil-Ojeda, M., Almansa,
F., Alonso-Pérez, S., Barreto, A., González-Morales, Y., Guirado-Fuentes, C., López-Solano, C., Afonso, S., Bayo, C.,
Berjón, A., Bethencourt, J., Camino, C., Carreño, V., Castro, N. J., Cruz, A. M., Damas, M., De Ory-Ajamil, F., García, M.

I., Fernández-de Mesa, C. M., González, Y., Hernández, C., Hernández, Y., Hernández, M. A., Hernández-Cruz, B., Jover, M., Kühl, S. O., López-Fernández, R., López-Solano, J., Peris, A., Rodríguez-Franco, J. J., Sálamo, C., Sepúlveda, E. and Sierra, M.: Izaña Atmospheric Research Center Activity Report 2012-2014. (Eds. Cuevas, E., Milford, C. and Tarasova, O.), State Meteorological Agency (AEMET), Madrid, Spain and World Meteorological Organization, Geneva, Switzerland, NIPO: 281-15-004-2, WMO/GAW Report No. 219, 2015.

EMPA: System and Performance Audit of Surface Ozone, Methane, Carbon Dioxide, Nitrous Oxide, and Carbon Monoxide at the Global GAW Station Izaña, September 2013, WCC-Empa Report 13/2, 62 pp, https://www.wmo.int/pages/prog/arep/gaw/documents/IZO_2013.pdf, 2013.

Gomez-Pelaez, A.J., Ramos, R.: "Improvements in the Carbon Dioxide and Methane Continuous Measurement Programs at Izaña Global GAW Station (Spain) during 2007-2009", in GAW report (No. 194) of the "15th WMO/IAEA Meeting of Experts on Carbon Dioxide, Other Greenhouse Gases, and Related Tracer Measurement Techniques (Jena, Germany; September 7-10, 2009)", edited by Willi A. Brand, World Meteorological Organization (TD No. 1553), Geneva, 133-138, 2011.

Gomez-Pelaez, A.J., Ramos, R., Gomez-Trueba, V., Campo-Hernandez, R., Dlugokencky, E., Conway, T.: "New improvements in the Izaña (Tenerife, Spain) global GAW station in-situ greenhouse gases measurement program" in GAW report (No. 206) of the "16th WMO/IAEA Meeting on Carbon Dioxide, Other Greenhouse Gases, and Related Measurement Techniques (GGMT-2011) (Wellington, New Zealand, 25-28 October 2011)", edited by Gordon Brailsford, World Meteorological Organization, Geneva, 76-81, 2012.

Gomez-Pelaez, A. J., Ramos, R., Gomez-Trueba, V., Novelli, P. C., and Campo-Hernandez, R.: A statistical approach to quantify uncertainty in carbon monoxide measurements at the Izaña global GAW station: 2008–2011, Atmos. Meas. Tech., 6, 787-799, https://doi.org/10.5194/amt-6-787-2013, 2013.

Gomez-Pelaez, A.J., Ramos, R., Gomez-Trueba, V., Campo-Hernandez, R., Reyes-Sanchez, E.: "Izaña Global GAW station greenhouse-gas measurement programme. Novelties and developments during October 2011-May 2013" in GAW report (No. 213) of the "17th WMO/IAEA Meeting on Carbon Dioxide, Other Greenhouse Gases, and Related Measurement Techniques (Beijing, China, June 10-14, 2013)", edited by P. Tans and C. Zellweger, World Meteorological Organization, Geneva, 77-82, 2014.

Gomez-Pelaez, A. J., Ramos, R., Gomez-Trueba, V., Campo-Hernandez, R., Reyes-Sanchez, E.: "GGMT-2015 Izaña station update: instrumental and processing software developments, scale updates, aircraft campaign, and plumbing design for CRDS" in GAW report (No. 229) of the "18th WMO/IAEA Meeting on Carbon Dioxide, Other Greenhouse Gases, and Related Measurement Techniques (GGMT) (La Jolla, CA, USA, 13-17 September, 2015)", edited by P. Tans and C. Zellweger, World Meteorological Organization, Geneva, 125-131, 2016.

Hazan, L., Tarniewicz, J., Ramonet, M., Laurent, O., and Abbaris, A.: Automatic processing of atmospheric CO2 and CH4 mole fractions at the ICOS Atmosphere Thematic Centre, Atmos. Meas. Tech., 9, 4719-4736, https://doi.org/10.5194/amt-9-4719-2016, 2016.

ICOS-ATC (Integrated Carbon Observation System, Atmospheric Thematic Center), "ICOS Atmospheric Station Specifications", edited by O. Laurent, version 1.2, 2016. https://icos-atc.lsce.ipsl.fr/filebrowser/download/27251

Karion, A., Sweeney, C., Wolter, S., Newberger, T., Chen, H., Andrews, A., Kofler, J., Neff, D., and Tans, P.: Long-term greenhouse gas measurements from aircraft, Atmos. Meas. Tech., 6, 511–526, doi:10.5194/amt-6-511-2013, 2013.

Patra, P. K., Krol, M. C., Montzka, S. A., Arnold, T., Atlas, E. L., Lintner, B. R., Stephens, B. B., Xiang, B., Elkins, J. W., Fraser, P. J., Ghosh, A., Hintsa, E. J., Hurst, D. F., Ishijima, K., Krummel, P. B., Miller, B. R., Miyazaki, K., Moore, F. L., Muhle, J., O'Doherty, S., Prinn, R. G., Steele, L. P., Takigawa, M., Wang, H. J., Weiss, R. F., Wofsy, S. C., Young, D.: Observational evidence for interhemispheric hydroxyl-radical parity, Nature, 513, 7517, 219-223, http://dx.doi.org/10.1038/nature13721, 2014.

Rella, C. W.: Accurate and stable carbon monoxide measurements with the Picarro G2302, Picarro Report, 2010.

Rella, C. W., Chen, H., Andrews, A. E., Filges, A., Gerbig, C., Hatakka, J., Karion, A., Miles, N. L., Richardson, S. J., Steinbacher, M., Sweeney, C., Wastine, B., and Zellweger, C.: High accuracy measurements of dry mole fractions of carbon dioxide and methane in humid air, Atmos. Meas. Tech., 6, 837–860, doi:10.5194/amt-6-837-2013, 2013.

Reum, F., Gerbig, C., Lavric, J. V., Rella, C. W., and Göckede, M.: An improved water correction function for Picarro greenhouse gas analyzers, Atmos. Meas. Tech. Discuss., https://doi.org/10.5194/amt-2017-174, in review, 2017.

Van den Bosch, C.J.H., Duijm, N.J.: "Outflow and spray release", in "Methods for the calculation of physical effects due to releases of hazardous substances (liquids and gases)", chapter 2, Third edition Second revised print, edited by C.J.H Van den Bosch and R.A.P.M. Weterings, The Netherlands Organization of Applied Scientific Research, The Hague, 2.1-2.179, 2005.

Rodríguez, S., González, Y., Cuevas, E., Ramos, R., Romero, P. M., Abreu-Afonso, J., and Redondas, A.: Atmospheric nanoparticle observations in the low free troposphere during upward orographic flows at Izaña Mountain Observatory, Atmos. Chem. Phys., 9, 6319-6335, https://doi.org/10.5194/acp-9-6319-2009, 2009.

WMO: 18th WMO/IAEA Meeting on Carbon Dioxide, Other Greenhouse Gases and Related Tracers Measurement Techniques (GGMT-2015), La Jolla, CA, USA, 13–17 September 2015, GAW Report No. 229, chap. Expert group recommendations, World Meteorological Organization, Geneva, Switzerland, 1–51, 2016.

Yver Kwok, C., Laurent, O., Guemri, A., Philippon, C., Wastine, B., Rella, C.W., Vuillemin, C., Truong, F., Delmotte, M., Kazan, V., Darding, M., Lebègue, B., Kaiser, C., Xueref-Rémy, I., and Ramonet, M.: Comprehensive laboratory and field testing of cavity ring-down spectroscopy analyzers measuring H2O, CO2, CH4 and CO, Atmos. Meas. Tech., 8, 3867–3892, doi:10.5194/amt-8-3867-2015, 2015.

Zellweger, C., Steinbacher, M., and Buchmann, B.: Evaluation of new laser spectrometer techniques for in-situ carbon monoxide measurements, Atmos. Meas. Tech., 5, 2555–2567, doi:10.5194/amt-5-2555-2012, 2012.

Zellweger, C., Emmenegger, L., Firdaus, M., Hatakka, J., Heimann, M., Kozlova, E., Spain, T. G., Steinbacher, M., van der Schoot, M. V., and Buchmann, B.: Assessment of recent advances in measurement techniques for atmospheric carbon dioxide and methane observations, Atmos. Meas. Tech., 9, 4737-4757, https://doi.org/10.5194/amt-9-4737-2016, 2016.